Cascadability of PPLN-Based Inter-Band Wavelength Conversion for Band-Switchable Multi-Band Optical Cross-Connect

Haruka Minami [1], Takafumi Fukatani [1], Masahiro Nakagawa [1], Takeshi Seki [1], Shimpei Shimizu [2], Takayuki Kobayashi [2], Takushi Kazama [2, 3], Koji Enbutsu [3], Takeshi Umeki [2, 3], Rie Hayashi [1], Takeshi Kuwahara [1]

1 NTT Network Service Systems Laboratories, NTT Corp. 3-9-11 Midori-cho, Musashino-shi, Tokyo, 180-8585, Japan
2 NTT Network Innovation Laboratories, NTT Corp. 1-1 Hikarinooka, Yokosuka, Kanagawa, 239-0547 Japan
3 NTT Device Technology Laboratories, NTT Corp. 3-1 Morinosato Wakamiya, Atsugi, Kanagawa 243-0198 Japan
haruka.minami@ntt.com

Abstract: A band-switchable multi-band optical cross-connect can contribute flexible operation of future multi-band networks. We review an experimental demonstration for cascadability of PPLN-based inter-band wavelength converters with a view to incorporating them into the optical cross-connect. © 2024 The Author(s)

1. Introduction

In response to the demand for transmission capacity expansion, multi-band (MB) wavelength-division multiplexing (WDM) transmission technology is attracting much attention because it can utilize existing optical fiber infrastructures [1, 2]. For early realization of MB transmission, all-optical inter-band wavelength converters (AO-WCs) effectively enable the use of wavelength bands unsupported by available devices. The inter-band wavelength conversion has been widely demonstrated using nonlinear effects such as a $\chi^{(3)}$-based four-wave mixing process [3–5] and a $\chi^{(2)}$-based differential frequency generation (DFG) process [6]. Furthermore, MB transmission demonstrations beyond conventional wavelength bands by using AO-WCs have been reported [7–9].

In MB networks, optical node systems that implement all-optical wavelength conversion technology are desirable to enable flexible operation. We have proposed a multi-band optical cross-connect (MB-OXC) incorporating AO-WCs, which can switch not only the output direction but also the output wavelength band of the input signals [10–12]. The band-switchable MB-OXC will be able to provide the following benefits in the applied network: 1) an increase in the traffic volume that can be accommodated by relaxing constraints on optical path design [11, 12] and 2) elimination of the need for optical-electrical-optical conversion when connecting a conventional single-band (SB) network or link with an MB one. Figure 1 shows two example scenarios where benefits 1) and 2) can be obtained by wavelength-band switching at MB-OXC 1 and 2, respectively. MB-OXC 1 permits the signals input from two directions even in the same wavelength band to be output in the same direction. MB-OXC 2 adapts input signals from the SB network to the MB network by selecting their output wavelength band. Figure 2 shows our proposed band-switchable MB-OXC architecture, consisting of AO-WCs and conventional OXC components. Since optical signals pass through multiple optical nodes in a network, the cascadability becomes an important requirement for the AO-WC incorporating into the MB-OXC. An AO-WC needs to be adopted that has little signal degradation even when optical signals pass through it many times to fully utilize the benefits of the MB-OXC.

Recently, we proposed a band-switchable MB-OXC configuration using AO-WCs based on periodically poled

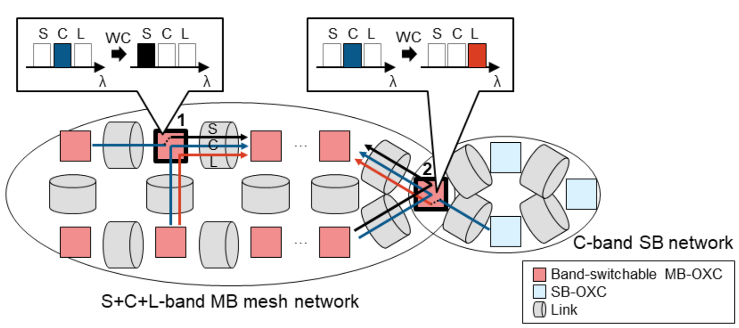

Fig.1. Examples of scenarios where the benefits of band-switchable MB-OXC can be obtained.

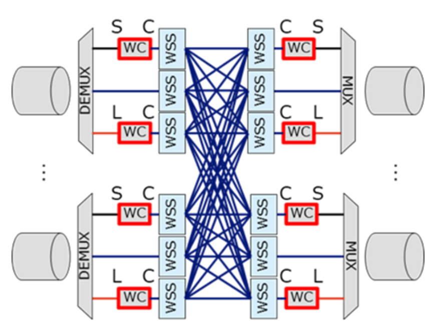

Fig.2. Band-switchable MB-OXC architecture supporting the S+C+L band.

lithium niobate (PPLN) waveguides and demonstrated its feasibility for C+L-band systems [13, 14]. In this paper, we review our recent investigation into the cascadability of the PPLN-based AO-WC for applying it to MB networks.

2. PPLN-based AO-WC

Figure 3 (a) shows a configuration of a C-to-L/L-to-C PPLN-based AO-WC. This is a polarization-diverse configuration sandwiched between two polarization beam splitters (PBSs). The PPLN waveguides for second-harmonic generation (SHG) convert a pump light at f_p (=190.6 THz, 1572.89 nm) to an SH pump light at $2f_p$. The PPLN waveguides for DFG generate an idler at $f_i = 2f_p - f_s$ for each polarization component, where a signal light at f_s is input. The filter on the output side extracts the idlers as wavelength-converted lights.

The PPLN-based AO-WC potentially has high cascadability suitable for constructing the MB-OXC because of its wide wavelength conversion bandwidth, high conversion efficiency (CE), low noise figure (NF), and low inter-channel crosstalk (XT). For simultaneous inter-band wavelength conversion, the bandwidth of nonlinear processes in an AO-WC should be 8–10 THz. Also, resistance to input pump power as well as nonlinear efficiency is important to achieve high CE. An AO-WC using directly bonded ZnO-doped PPLN ridge waveguides enables wideband WDM signals to be converted simultaneously with high CE thanks to the high $\chi^{(2)}$-nonlinearity, quasi-phase-matching, high resistance to pump power, and its large light-confining effect [15]. In addition, a 4-port PPLN module, in which connection parts between the fiber and waveguide and dichroic mirrors for pump (de-)combining are integrated, provides low excess loss and low NF [16, 17]. As shown in Fig. 3 (b), the C-to-L/L-to-C PPLN-based AO-WC was able to provide CE of ~10 dB and NF of ~5 dB regardless of C-to-L and L-to-C conversions, with the SH pump power of ~30 dBm. Furthermore, the low inter-channel XT can be achieved by adopting a two-stage configuration using different PPLNs for SHG and DFG, and thus, the input power tolerance for the wideband WDM signal can be improved [18, 19]. The gain saturation due to pump depletion is still one of the factors limiting the input signal power, and its effect on signal quality has been experimentally investigated [14, 20]. The saturated gain causes the nonlinear signal distortion due to the ultrafast response of a wavelength conversion process. Although the total input power increases with the number of WDM channels, the effect of gain saturation on signal distortion has been reported to be suppressed for a wideband WDM signal [14, 20].

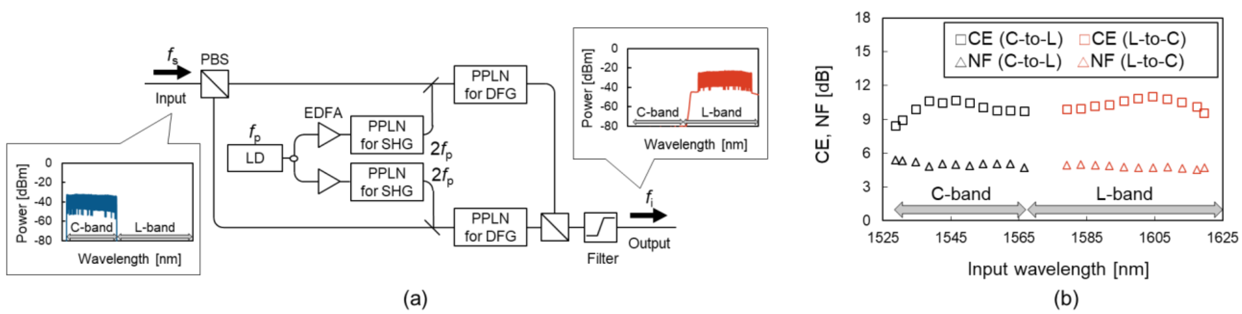

Fig. 3 (a) Configuration and (b) CE and NF characteristics of C-to-L/L-to-C PPLN-based AO-WC.

3. Experimental evaluation on cascadability of PPLN-based AO-WC

Optical signal-to-noise (OSNR) degradation due to amplified spontaneous emission (ASE) noise and the signal distortion caused by gain saturation depend on the input signal power to the PPLN-based AO-WC. Thus, we investigated the optimal input power condition to achieve better signal quality with multiple wavelength-band conversions in a recirculating loop experiment [13, 14]. Figure 4 (a) shows the experimental setup. The transmitted C-band 50-GHz-spacing 96-channel WDM signal consisted of the measurement channel, which was modulated by 32-Gbaud DP-16QAM, and the dummy WDM channels generated with the ASE light output from an erbium-doped fiber amplifier (EDFA). The signal was transmitted over a 40-km single-mode fiber (SMF) loop with the launch power of −11 dBm/ch (fiber-nonlinearity was negligible) and was wavelength converted twice by the C-to-L and L-to-C AO-WCs in each lap. To evaluate the signal quality, the SNR was calculated from the variance of the recovered symbols by offline digital signal processing. Figure 4 (b) shows dependence of SNR on input power per channel to the PPLN-based AO-WCs when the numbers of traversed AO-WCs were 2, 10, and 20. The dotted lines show the calculated SNRs considering only linear ASE noise accumulated with the recirculating, i.e., indicating the signal quality in the case without nonlinear penalty. While the calculated SNR improved as the input power increased, the measured SNR was maximum at around −10 dBm/ch because of the gain saturation. The optimal input powers were almost independent of the number of the traversed AO-WCs when it was within 20. These results show that operating the PPLN-based AO-WC at the optimal input power determined by the balance between the received OSNR improvement and the nonlinear penalty contributes to ensuring the cascadability.

Moreover, we successfully confirmed that the PPLN-based AO-WCs can achieve the cascadability required to improve accommodated traffic volume by the band-switchable MB-OXCs [14]. According to our numerical investigation [12], it is expected that fiber resources can be reduced by > 20% thanks to the increase in accommodated traffic volume as long as the generalized SNR (GSNR) penalty per wavelength-band conversion is suppressed to < 0.7 dB. We compared the experimentally measured SNRs under the optimal input power condition with the lower SNR limits assuming the GSNR penalty of 0.7 dB per wavelength-band conversion. As shown in Fig. 4 (c), the measured SNR exceeded the lower SNR limit for all numbers of traversed PPLN-based AO-WCs. Assuming that the number of traversed AO-WCs within one MB-OXC is 2 (see Fig. 2) and average number of hops between node pairs is ~6 in the backbone network [21], the possible number of traversed AO-WCs is ~12. Thus, the number of AO-WC traverses of 24, which is the maximum number measured experimentally, is sufficient for realistic conditions.

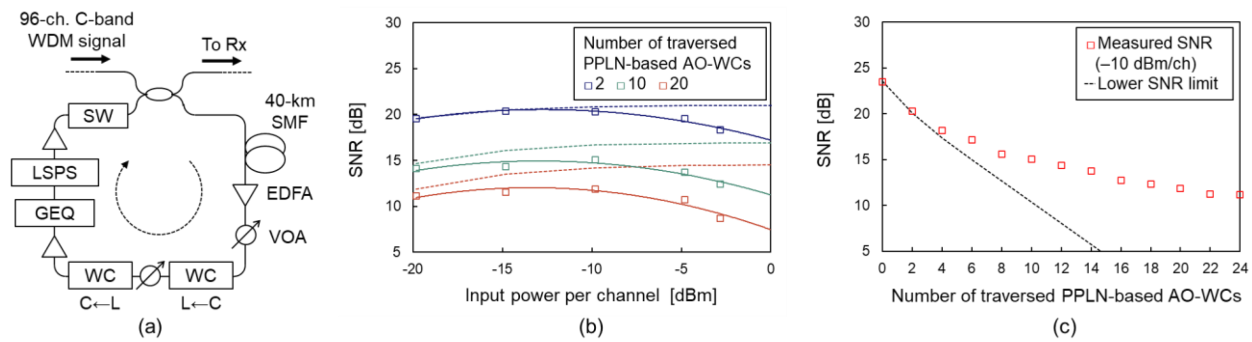

Fig. 4 (a) Experimental setup. VOA: variable optical attenuator, GEQ: gain equalizer, LSPS: loop-synchronous polarization scrambler, and SW: optical switch. (b) Dependence of measured and calculated SNR on the input power to PPLN-based AO-WCs. (c) Measured SNRs at the optimal input power per channel and calculated lower SNR limits to increase in accommodated traffic volume by band switching.

4. Conclusion

This paper described our recent proposal of applying PPLN-based AO-WCs to a band-switchable MB-OXC. The cascadability of the PPLN-based AO-WC shown in the experiments was sufficient to fully bring out the benefits of the band-switchable MB-OXC. Future developments for practical use in PPLN-based all-optical wavelength conversion will accelerate the realization of the MB-OXC. We believe that such an optical node system utilizing all-optical signal processing will contribute to flexible and economical MB networks.

References

[1] F. Hamaoka *et al.*, J. Lightwave Technol., **37**, 8, 1764–1771 (2019).
[2] B. J. Puttnam *et al.*, in Proc. ECOC2023, Paper Th.C.2.4 (2023).
[3] T. Kato *et al.*, in Proc. OFC2021, Paper F1B.1 (2021).
[4] I. Sackey *et al.*, in Proc. ECOC2021, Paper We4C1.5 (2021).
[5] P. Zhao *et al.*, Nanophotn., **12**, 17, 3427-3434 (2023).
[6] S. Shimizu *et al.*, J. Lightwave Technol., **40**, 11, 3374–3384 (2022).
[7] T. Kato *et al.*, in Proc. ECOC2022, Paper We4D.4 (2022).
[8] D. Soma *et al.*, in Proc. ECOC2023, Paper Th.C.2.2 (2023).
[9] M. Abe *et al.*, in Proc. FiO+LS2023, Paper FM5D.2 (2023).
[10] H. Kawahara *et al.*, in Proc. ECOC2020, Paper Tu1H-5 (2020).
[11] M. Nakagawa *et al.*, in Proc. ONDM2021 (2021).
[12] M. Nakagawa *et al.*, IEICE Trans. Commun., **E106-B**, 5, 416–426 (2023).
[13] H. Minami *et al.*, in Proc. OFC2023, Paper M4G.1 (2023).
[14] H. Minami *et al.*, J. Lightwave Technol., to be published. DOI: 10.1109/JLT.2023.3302475.
[15] T. Umeki *et al.*, J. Quantum Electron. **46**, 8, 1206–1213 (2010).
[16] T. Kazama *et al.*, Opt. Express, **29**, 18, 28824–28834, (2021).
[17] T. Kashiwazaki *et al.*, Appl. Phys. Lett., **119**, 251104, 416–426 (2021).
[18] T. Kazama *et al.*, J. Lightwave Technol., **35**, 4, 755–761 (2017).
[19] M. Asobe *et al.*, Electron. Lett., **45**, 10, 519 (2009).
[20] S. Shimizu *et al.*, J. Lightwave Technol., **41**, 15, 4922–4932 (2023).
[21] K. Ishii *et al.*, J. Lightwave Technol., **33**, 21, 4395–4405 (2015).